Assessment of Turbulence Models for Flow around Three-dimensional Geometries

Emmanuel Guilmineau, Ganbo Deng, P. Queutey, Michel Visonneau, J. Wackers

Assessment of Turbulence Models for Flow around Three-dimensional Geometries

E. Guilmineau, G.B. Deng, P. Queutey, M. Visonneau and J. Wackers

Abstract This paper presents a computational study of flow around three-dimensional geometries as the Ahmed body, which is a classical test case for automotive flow, but also as the JBC (Japan Bulk Carrier) which was first investigated in the framework of the Tokyo 2015 Workshop on Numerical Ship Hydrodynamics. For both test cases, an investigation of RANS ($k-\omega$ SST and EARSM) and hybrid RANS-LES models (DES and IDDES) is conducted. All simulations have been performed with the ISIS-CFD flow solver, which is developed by Ecole Centrale de Nantes and CNRS. For both geometries, the hybrid RANS-LES models predict a high level of turbulent kinetic energy which is in better agreement with the experiments than the quantity predicted with a RANS turbulence model.

1 Introduction

The prediction of the velocity field in the wake of a body is one of the most important problems. For an automotive flow, the separated wake flow contributes to the drag and thus influences the fuel efficiency of the vehicle. For a ship flow, the a nonuniform velocity field in the wake causes some variations of the propeller thrust in time and thus strong vibrations in the stern area.

Numerical simulation of the wake of a three-dimensional body has been a subject of study for a long time. An important feature of the works done is the use of the URANS (unsteady Reynolds averaged Navier-Stokes) method which can capture the steady effects and the large scale unsteadiness. Unfortunately, the URANS approach is not able to capture many unsteady effects caused by vortices in the wake of three-dimensional bodies. Therefore, the application of vortex resolving methods, like LES (large eddy simulation) is necessary. But a pure LES is still impossible due to the high computational resources which are necessary, see Nishikawa [13] who

LHEEA, CNRS UMR 6598, Ecole Centrale de Nantes, e-mail: Emmanuel.Guilmineau@ec-nantes.fr

uses a mesh with 38×10^9 cells to simulate the flow around a ship. So, hybrid RANS-LES approaches seem to be a good alternative to solve problems with reasonable computer resource consumption.

In this paper, two geometries are investigated. The first is a generic car model, the Ahmed body [2]. The second is a ship hull, the Japan Bulk Carrier (JBC) which is used as one of the test-cases of the Tokyo 2015 workshop [1] on Numerical Ship Hydrodynamics. All the computations which are presented in this paper are performed with the flow solver ISIS-CFD.

2 Test cases

2.1 The Ahmed body

The Ahmed body, shown in Figure 1, is a generic car comprising a flat front with rounded corners and a shaped slanted rear upper surface. The length of the model is L = 1044 mm, its height is H = 288 mm and its width = 389 mm. The ground clearance is 50 mm. The diameter of the four feet, which are used to secure the model to the floor of the wind tunnel, is 30 mm. The slant angle is adjustable and is the main variable model-parameter in the experimental investigations of Ahmed et al. [2]. In this paper, only the 25° slant angle is investigated. The Reynolds number, Re = 7.68×10^5, is based on the height of the model and the incoming velocity, U_∞ = 40 m/s.

Fig. 1 Ahmed - Geometry

The computational domain starts 2L in front the model and extends to 5L behind the model. The width is 1.87 m and the height is 1.4 m. The mesh is generated using Hexpress™, an automatic unstructured mesh generator. This software generates meshes containing only hexahedrals. For the surface of the car model and the floor, a no-slip boundary condition is used and the wall normal resolution is set to 0.0007 mm, i.e. $y^+ \leq 0.7$. The mesh consists of 23.1×10^6 cells and the model is described by 384,000 faces. To capture the unsteadiness of the flow, an unsteady simulation is carried out with the RANS turbulence models. In this case, the time step is $\Delta t = 10^{-3}$ s and the numerical simulation converges to a steady flow. With

the hybrid RANS-LES models, the flow is by nature unsteady and the time step is $\Delta t = 2.5\times10^{-4}$ s. The non-dimensional averaging time, $t\times U_\infty/H$, in the simulation is 150.

2.2 The Japan Bulk Carrier

The Japan Bulk Carrier (JBC) is a Capesize bulk carrier, represented in Figure 2. Its length between perpendiculars at full scale is L_{PP} = 280 m and its service speed is 14.5 knots, leading to a Froude number Fn = 0.142. The depth is 25 m and the draft is 16.5 m. This geometry is investigated at model scale, where its length is L_{PP} = 7 m and the Reynolds number is Re = 7.46×10^6, based on the length L_{PP} and the velocity U = 1.179 m/s.

Fig. 2 JBC - Geometry

The computational domains starts $2L_{PP}$ in front the model ans extends to $5L_{PP}$ behind the hull. The width is 4 m and the height is $2.06L_{PP}$. The free-surface effects are not taken into account and thus this plane is a symmetry plane. This configuration is called double-body. This mesh is also generated by Hexpress™and the grid around the complete double-body hull is comprised of 66×10^6 cells. The hull is described by 473,198 faces. For the RANS simulations, the time step is $\Delta t = 6\times10^{-2}$ s and the averaging time, $t\times U$/Lpp, is 15.3. For the hybrid RANS-LES simulations, the time step is $\Delta t = 6\times10^{-3}$ s and the averaging time is 24.2.

3 ISIS-CFD at glance

ISIS-CFD, developed by the Ecole Centrale de Nantes and CNRS and available as a part of the FINE™/Marine computing suite, is an incompressible unsteady Reynolds-averaged Navier-Stokes (URANS) method. The solver is based on the finite volume method to build the spatial discretization of the transport equations. The unstructured discretization is face-based, which means that cells with an arbitrary number of arbitrarily shaped faces are accepted. A second order backward difference scheme is used to discretize time. The solver can simulate both steady and unsteady flows. The velocity field is obtained from the momentum conservation equations and the pressure field is extracted from the mass equation constraint, or continuity equation, transformed into a pressure equation. In the case of turbu-

lent flows, transport equations for the variables in the turbulence model are added to the discretization. A detailed description of the solver is given by Queutey and Visonneau [14].

The solver features sophisticated turbulence models: apart from the classical two-equation k-ε and k-ω models, the anisotropic two-equation Explicit Algebraic Reynolds Stress Model (EARSM), as well as Reynolds Stress Transport Models, are available, see Duvigneau et al. [4] and Deng and Visonneau [3]. All these are RANS models. A Detached Eddy Simulation (DES) approach, based on Menter et al. [11], has been introduced, see Guilmineau et al. [6]. Recently, some modifications of this formulation proposed by Griskevich et al. [5] include recalibrated empirical constants in the shielding function and a simplification of the original Spalart-Allmaras-based formulation. This new model is called Improved Delayed Detached Eddy Simulation (IDDES).

4 Results

4.1 The Ahmed body

Figure 3 shows the vortex structures by using a dimensionless iso-surface of λ_2. With the RANS models, a massive separation is predicted. The results obtained with the $k-\omega$ SST contain the C-pillar vortices but these vortices are not enough strong to prevent the massive separation. With the hybrid RANS-LES models, the C-pillar vortices are predicted, but they are more pronounced with the IDDES approach which is the only turbulence model to predict the separation bubble on the slanted surface.

Figure 4 presents the friction lines on the walls of the model. With the EARSM turbulence model, the flow is fully separated on the slant while with the $k-\omega$ SST model, the flow is separated on the slant but a vortex is also predicted at the level of the lateral edge of the model. With a hybrid RANS-LES model, the sketch on the rear slant is approximately the same. The major difference is the position of the reattachment of the bubble on the slant. The flow predicted with IDDES separates at the front end of the body. This separation at the beginning of the roof has already been noted experimentally [15] but also numerically [8, 12].

A comparison of the streamwise velocity component on the slanted surface and in the wake is presented in Figure 5. The experimental profiles are those obtained by Lienhart and Becker [9]. As expected by the previous figure, the agreement with the experiments on the slant is not good for the results obtained with the RANS turbulence models. The hybrid RANS-LES approaches provide a good estimation of the boundary layer thickness at the end of the roof. Moreover, with the IDDES model, the boundary layer thickness becomes less thick that than obtained with the DES model which is in better agreement with the experiments. In the wake of the model, as the RANS turbulence models predict a massive separation, the agreement

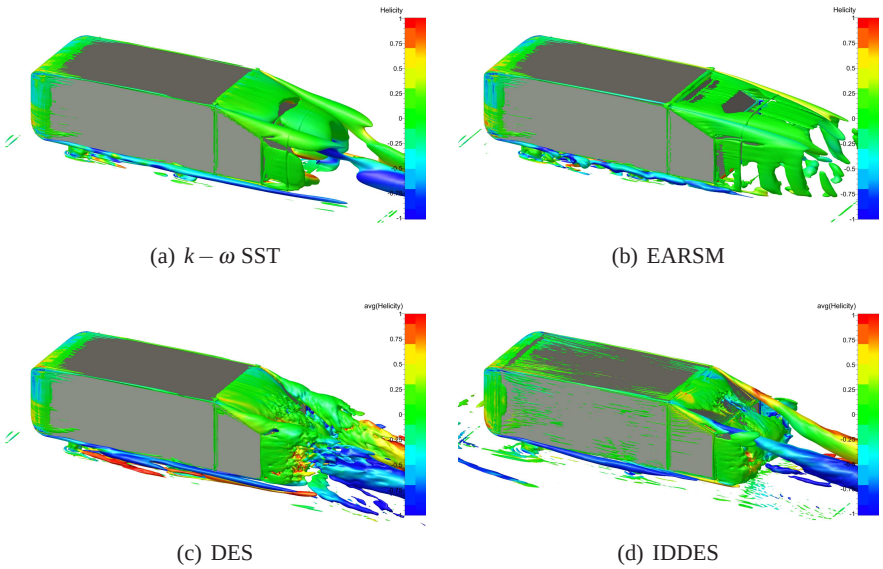

(a) $k-\omega$ SST (b) EARSM

(c) DES (d) IDDES

Fig. 3 Ahmed - Vortex structures around the Ahmed body visualized by an iso-surface of dimensionless λ_2 (λ_2=0.76)

with the experimental data is not good. With the hybrid RANS-LES models, as the separation is smaller, the results are in better agreement with the experiments. The results obtained with the IDDES approach match very well the experimental data.

Figure 6 presents a comparison between experimental and numerical turbulent kinetic energy (TKE) in the symmetry plane. With the RANS turbulence models, the results are underestimated just after the upper edge of the rear slant surface. This means less turbulent mixing and thus a greater recirculation region. With the hybrid RANS-LES models, the TKE is overestimated, particularly at the end of the slanted surface. However, at the first X-position on the slant, the results obtained with the IDDES model are in relatively good agreement with the experimental data. In the wake of the model, as the hybrid RANS-LES approaches give a recirculation in better agreement with the experiments, the comparison of the TKE profiles matches the experimental data.

The force coefficients, the drag and the lift, are presented in Table 1 for all turbulence models. The values measured by Ahmed et al. [2] are also indicated as well as those measured by Meile et al. [10] and by Thacker et al. [16] for the same Reynols number used in this paper. There are significant differences between all numerical simulations, it is not surprising that the drag coefficient varies depending of the turbulence model used. Even in the experiments, the drag value is not the same. The drag coefficient obtained with the IDDES model is in good agreement with the drag measured by Thacker et al. [16]. The lift coefficient has the same order of magnitude

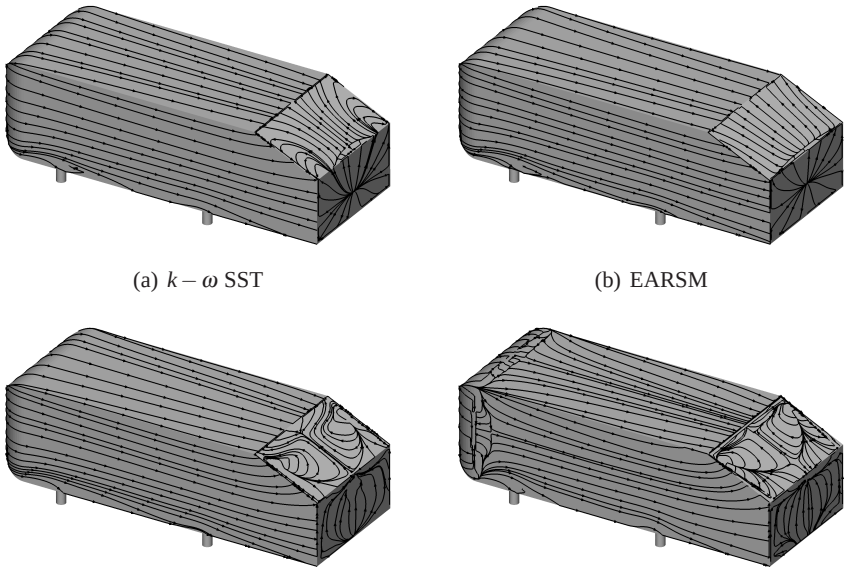

(a) $k-\omega$ SST (b) EARSM

(c) DES (d) IDDES

Fig. 4 Ahmed - Friction lines on the model

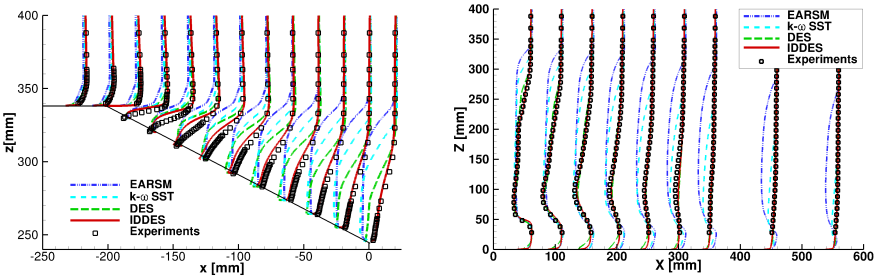

(a) On the slanted surface (b) in the wake

Fig. 5 Ahmed - Comparison of the streamwise velocity component in the symmetry plane

with the hybrid RANS-LES models while with the RANS models this coefficient is lower, and particularly with the EARSM model.

Table 1 Ahmed - Drag and lift coefficients

	$k-\omega$ SST	EARSM	DES	IDDES	Experiments [2]	Experiments [10]	Experiments [16]
C_D	0.3218	0.2804	0.4371	0.3802	0.2850	0.2990	0.3840
C_L	0.1724	0.0083	0.3747	0.3306	n.a.	0.3450	0.4220

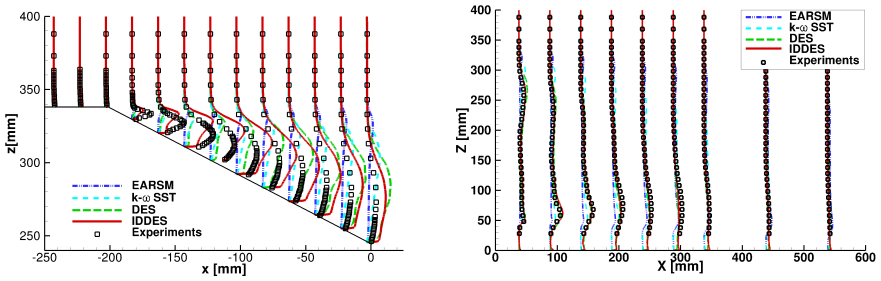

(a) On the slanted surface (b) in the wake

Fig. 6 Ahmed - Comparison of the turbulent kinetic energy profiles in the symmetry plane

4.2 The Japan Bulk Carrier

Figure 7 presents the vortex structures by using a dimensionless iso-surface of Q obtained with the EARSM turbulence model. A massive vortex is observed in the wake of the hull. This topology is the same with the DES for the mean flow.

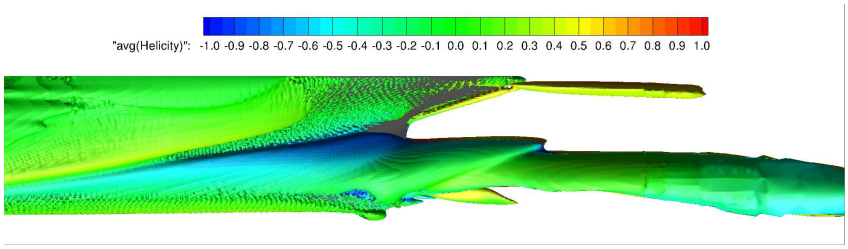

Fig. 7 JBC - Side view of the vortical structures visualized by iso-surface of dimensionless Q (Q=25)

A local vortex core analysis is performed only on the main vortex. To define the main vortex center, one usually relies on the local maximum value of the second invariant Q in order to keep a physical consistency. The transversal evolutions along horizontal and vertical lines across the vortex center are computed for the cross-section S4, located at $X/L_{PP} = 0.9843$. The coordinates of the mean vortex center in this plane are called Y_{V1} and Z_{V1}.

Figures 8 and 9 show the comparison of the longitudinal component of the velocity, U, and the turbulent kinetic energy, TKE, respectively, between the numerical results and the experimental data. A satisfactory agreement is observed for the mean streamwise velocity component while a large difference between the experimental data and the numerical results for TKE is noticed. During the T2015 workshop [17], this trend was found by all the participants using RANS turbulence models. The result obtained with the DES is in agreement with the results obtained by Kornev's

team [7] who used a hybrid RANS-LES turbulence model. With the hybrid RANS-LES formulation, the level of TKE is in very good agreement with measurements and is three to ten times higher than what is simulated by the anisotropic RANS model. From a RANS point of view, the co-existence of high levels of TKE and large levels of longitudinal vorticity in the core of a vortex is somewhat contradictory, since high levels of TKE mean even higher levels of turbulence viscosity which contributes to the dissipation of the vortex and consequently reduces its vorticity. This point of view is valid if we are in presence of a unique isolated vortex, but the unsteady DES computations reveal that an isolated bilge vortex for the JBC is actually a kind of intellectual reconstruction which does not reflect the physical reality.

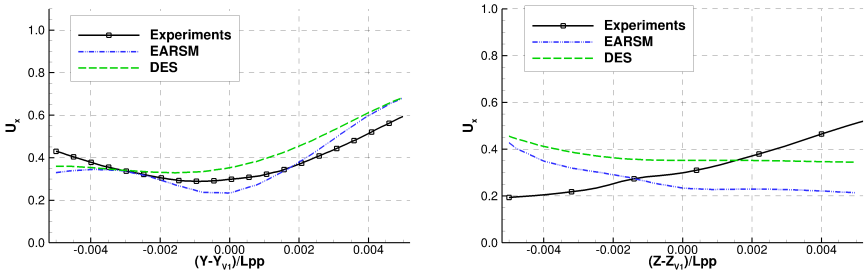

(a) Horizontal evolution (b) Vertical evolution

Fig. 8 JBC - Evolution of the streamwise velocity component around the vortex center

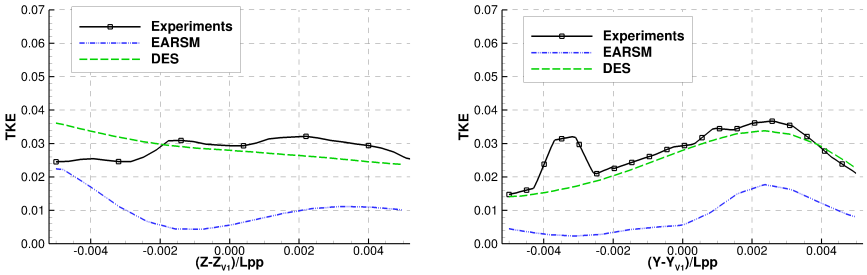

(a) Horizontal evolution (b) Vertical evolution

Fig. 9 JBC - Evolution of the turbulent kinetic energy around the vortex center

The averaged bilge vortex obtained is actually a superposition of intense and strongly unsteady smaller vortical structures, as shown in Figure 10 which provides two instantaneous views of the longitudinal vorticity, obtained by DES, at section S4 separated by ten time steps, i.e. 0.06 s. This may explain the large levels of

averaged TKE and the longitudinal vorticity. The unsteady motion of these smaller scale vortical structure contributes to a high level of TKE which is associated with relatively low frequency fluctuations.

ls 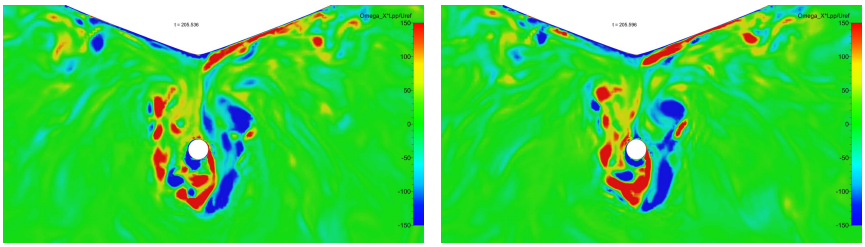

(a) Time 205.536 s (b) Time 205.596 s

Fig. 10 JBC - Instantaneous views of the longitudinal vorticity

An instantaneous view of the iso-surface of the second invariant Q, not presented in this paper, shows a succession of ring vortices which are created after the onset of an open separation linked with the initial thickening of the boundary layer illustrated by the convergence of the averaged friction lines. This large scale unsteadiness is likely to be due to the design of JBC with a large value of the block coefficient C_B, $C_B = 0.858$. The rapid reduction of the hull sections at the stern, implied by the high value of C_B, creates the condition of open separation followed by a flow reversal and a strong unsteadiness revealed by the shedding of ring vortices.

5 Conclusions

This paper presents an investigation of RANS and hybrid RANS-LES models for two types of flow. The first is aerodynamics with the Ahmed body at a 25° slant angle. The second is hydrodynamics with the hull of the Japan Bulk Carrier.

For the Ahmed body, the numerical results are highly dependent on the turbulence model used. The RANS approach fails to capture the separation on the slant. The IDDES hybrid RANS-LES model is the only one that predicts correctly the bubble on the slant. Therefore, the velocity profiles and the turbulent kinetic energy are in agreement with the experimental data.

For the JBC, the hybrid RANS-LES computations show a marked unsteady separation zone characterized by a wake of coherent ring-vortices periodically shed at the stern of the ship. These numerical simulations provide a new interpretation of the averaged stern flow which removes the contradiction between high levels of vorticity and turbulent kinetic energy in the core of the averaged vortex.

Acknowledgements This work was granted access to the HPC resources of CINES/IDRIS under the allocations 2015-2a0129 and 2016-2a0129 made by GENCI.

References

1. http://www.t2015.nmri.go.jp/
2. Ahmed, S.R., Ramm, G., Faltin, G.: Some salient features of the time-averaged ground vehicle wake. SAE World Congress (1984). Paper 840300
3. Deng, G.B., Visonneau, M.: Comparison of explicit algebraic stress models and second-order turbulence closures for steady flow around ships. In: 7th Symposium on Numerical Ship Hydrodynamics, pp. 4.4–1–15. Nantes, France (1999)
4. Duvigneau, R., Visonneau, M., Deng, G.B.: On the role played by turbulence closures in hull ship optimization at model and full scale. Journal of Marine Science and Technology **8**, 11–25 (2003)
5. Gritskevich, M.S., Garbaruk, A.V., Schütze, J., Menter, F.R.: Development of DDES and IDDES formulations for the k-ω shear stress transport model. Flow, Turbulence and Combustion **88**, 431–449 (2012)
6. Guilmineau, E., Deng, G.B., Wackers, J.: Numerical simulation with a DES approach for automotive flows. Journal of Fluids and Structures **27**, 807–816 (2011)
7. Kornev, N., Taranov, A., Shchukin, E., Kleinsorge, L.: Development of hybrid URANS-LES methods for flow simulation in the ship stern area. Ocean Engineering **38**, 1831–1838 (2011)
8. Krajnović, S., Davidson, L.: Flow around a simplified car - part 1: Large eddy simulation. Journal of Fluids Engineering **127**, 907–918 (2005)
9. Lienhart, H., Becker, S.: Flow and turbulence in the wake of a simplified car model. SAE World Congress (2003). Paper 2003-01-0656
10. Meile, W., Brenn, G., Reppenhagen, A., Lechner, B., Fuchs, A.: Experiments and numerical simulations on the aerodynamics of the Ahmed body. CFD Letters **3**(1), 32–39 (2011)
11. Menter, F.R., Kuntz, M., Langtry, R.: Ten years of industrial experience with the SST turbulence model. In: K. Hanjalić, Y. Nagano, M. Tummers (eds.) Turbulence, Heat and Mass Transfer 4, vol. 19, pp. 339–352. Begell House, Inc. (2003)
12. Minguez, M., Pasquetti, R., Serre, E.: High-order large eddy simulation of flow over the "Ahmed body" car model. Physics of Fluids **20** (2008)
13. Nishikawa, N.: Application of fully resolved large eddy simulation to Japan bulk carrier with an energy saving device. In: Tokyo 2015 Workshop on CFD in Ship Hydrodynamics. Tokyo, Japan (2015)
14. Queutey, P., Visonneau, M.: An interface capturing method for free-surface hydrodynamic flows. Computers and Fluids **36**, 1481–1510 (2007)
15. Spohn, A., Gilliéron, P.: Flow separations generated by a simplified geometry of an automotive vehicle. In: IUTAM Symposium on Unsteady Separated Flows. Toulouse, France (2002)
16. Thacker, A., Aubrun, S., Leroy, A., Devinant, P.: Effects of suppressing the 3D separation on the rear slant on the flow structures around the Ahmed body. Journal of Wind Engineering and Industrial Aerodynamics **107–108**, 237–243 (2012)
17. Visonneau, M.: JBC local flow analysis. In: Tokyo 2015 Workshop on CFD in Ship Hydrodynamics. Tokyo, Japan (2015)